Static Space Charge and Capacitance for a Single Blocking Electrode*

J. Ross Macdonald

Texas Instruments Incoprorated, Dallas 9, Texas

(Received April 21, 1958)

Static space-charge distributions in materials having one charge blocking and one ohmic electrode are considered with special emphasis on the situation where charge carriers of only one sign are mobile but which may recombine bimolecularly with fixed charges of opposite sign. The dependence of potential, charge, and electric field on distance from the blocking electrode cannot be obtained exactly in closed form but various simple approximate relations are obtained and are compared with accurate digital computer solutions of the exact relation between potential and distance. Comparison is most significant when the distance scale is normalized by the effective Debye length, a quantity which is shown to depend on recombination ratio when charges of only one sign are mobile. The dependence of total space-charge and differential and static space-charge capacitance on applied potential and recombination is obtained in closed form, and it is shown that recombination can lead to peaks in the curves of static and differential capacitance *versus* applied potential. Observation of these peaks should afford a simple method of determining recombination ratio and other pertinent parameters of the material. Finally, the addition of a charge-free layer in series with the space-charge region is considered, and the effect of such addition on differential capacitance investigated. The combination of a charge-free layer and space-charge region represents a combination of Mott's and Schottky's theories of rectification insofar as capacitance effects are concerned and is therefore pertinent to measurements on barrier-layer rectifiers as well as to material with a completely blocking electrode.

INTRODUCTION

WHENEVER the motion of electric charge in a solid or liquid under the influence of an electric field is partly or completely impeded at an electrode, a space-charge region forms near the electrode. Measurement of the spatial dependence of potential within the material and of the space-charge capacitance as functions of applied external potential can yield valuable information concerning the nature and concentrations of charge carriers within the material, and of recombination and breakdown properties. When mobile charge cannot leave or enter the charge-containing material at an electrode, this electrode may be termed blocking for such charge. Although this condition is strictly an idealization, it is one which is often well approximated experimentally, as discussed later. An ohmic contact or electrode may be thought of as the opposite of a blocking electrode. Formally, an ohmic contact may be defined as one in which the Fermi level in the electrode material is equal to that in the charge-containing material adjoining it before as well as after contact between them. Practically, this means that there is no potential drop at the junction of the two materials in the range of applied potentials over which the contact is ohmic.

The static space-charge distributions for material containing mobile, univalent, noncombining positive and negative charges have been obtained for a single completely blocking electrode[1] and for material between two such electrodes.[2,3] In the present paper, a solution of the one-electrode case will be given when charge of only one sign is mobile but can recombine with fixed charge of opposite sign. In a succeeding paper, the similar case with two blocking electrodes will be treated. A small-signal linearized theory of the ac response of such a system has already been given.[4]

There are many experimental situations in solids where it is more likely that charge of only a single sign is mobile than that charges of both signs move. Even in the latter case when the two mobilities are widely different a quasi-static distribution will be initially set up which will be like that occurring when charge of only one sign is mobile.[3] Examples of materials for which the present treatment is likely to apply when one or more blocking electrodes are used are: photoconducting alkali and silver halides,[5–8] impure ice,[9] plastic insulators,[10] electrets,[11] and glass.[12,13] Finally, the treatment will apply, at least approximately, to extrinsic semiconductors. It should be emphasized that the univalent charges considered need not be electrons or holes but can be protons, other ions, charged impurities, vacancies, etc.

The mobile charge with which we shall be concerned is assumed to arise from ionization of neutral impurity centers in the material and from injection at any nonblocking electrode. When injection or extraction occurs, the material as a whole will not be neutral. Ionization may take place thermally, by the absorption

* Presented in part at the Washington, D. C., meeting of the American Physical Society, May 3, 1958 [J. R. Macdonald, Bull. Am. Phys. Soc. Ser. II, **3**, 218 (1958)].

[1] J. R. Macdonald and M. K. Brachman, J. Chem. Phys. **22**, 1314 (1954).

[2] G. Jaffé, Ann. Physik **16**, 217 (1933).

[3] J. R. Macdonald, J. Chem. Phys. **22**, 1317 (1954).

[4] J. R. Macdonald, Phys. Rev. **92**, 4 (1953).

[5] R. J. Friauf, J. Chem. Phys. **22**, 1329 (1954).

[6] J. R. Macdonald, Phys. Rev. **85**, 381 L (1952); J. Chem. Phys. **23**, 275 (1955).

[7] Von Hippel, Gross, Jelatis, and Geller, Phys. Rev. **91**, 568 (1953).

[8] F. C. Brown, J. Phys. Chem. Solids **4**, 206 (1958).

[9] Gränicher, Jaccard, Scherrer, and Steinemann, Discussions Faraday Soc. No. **23**, 50 (1957).

[10] R. J. Munick, J. Appl. Phys. **27**, 1114 (1956).

[11] B. Gross, J. Chem. Phys. **17**, 866 (1949).

[12] J. E. Stanworth, *Physical Properties of Glass* (Oxford University Press, London, 1953).

[13] B. Gross, Phys. Rev. **107**, 368 (1957).

of radiation, or under the influence of high electric fields. We shall assume for simplicity that there are no neutral traps in the material which can capture mobile charge and become charged but that all recombination is bimolecular between mobile charge and ionized impurity centers. Some time ago it was pointed out that the present case was of interest but that it could not be solved completely in closed form.[3] With the recent availability to the author of an IBM 650 computing machine, presentation of accurate solutions to the equations then considered has become possible and pertinent.

SOLUTIONS FOR A SINGLE BLOCKING ELECTRODE

Let us consider unit cross section of charge-containing material extending from a plane, blocking electrode at $x=0$ to $+\infty$. It will be assumed that the electrode at infinity is essentially ohmic so that mobile charge can enter or leave the material there without space-charge formation. As we shall see later, the assumed semi-infinite length in practice need amount to only a few effective Debye lengths and the ohmic electrode need not be entirely ohmic for the theory to still hold.

For simplicity, we shall specify that any blocking-electrode contact or surface potential shall be included in the applied potential ψ_0, making the internal potential ψ an inner potential. Thus, when ψ is zero throughout the material, it will be electrically neutral throughout.† Discussions of inner and electrochemical potential pertinent to the present case have been given by Skinner[14] and Graham.[15]

The pertinent differential equations for charge motion under the influence of an electric field in a solid or liquid may be written for a one-dimensional system with bimolecular recombination as[4]

$$\partial n/\partial t = k_1 n_c - k_2 np + D_n(\partial^2 n/\partial x^2) + \mu_n[\partial(nE)/\partial x], \quad (1)$$

$$\partial p/\partial t = k_1 n_c - k_2 np + D_p(\partial^2 p/\partial x^2) - \mu_p[\partial(pE)/\partial x], \quad (2)$$

$$\partial n_c/\partial t = -k_1 n_c + k_2 np, \quad (3)$$

$$\partial E/\partial x = (4\pi e/\epsilon)(p-n), \quad (4)$$

$$E = -d\psi/dx. \quad (5)$$

In these equations, n_c is the concentration of neutral impurity centers, k_1 and k_2 are dissociation and recombination rate constants, and the other symbols have their conventional meanings. The condition that both positive and negative charge be blocked at an electrode is that of zero positive and negative currents.

$$\left.\begin{aligned} \mu_p pE - D_p(\partial p/\partial x) &= 0 \\ \mu_n nE + D_n(\partial n/\partial x) &= 0 \end{aligned}\right\} \text{at electrode.} \quad (6)$$

Let us now specialize the foregoing equations for the static case and for negative charges only mobile. Note that in the static case, the dielectric constant ϵ in (4) is the low-frequency limiting value of the differential dielectric constant of the material in the absence of free charges.[16] As long as the dielectric constant is independent of field strength, the static and differential dielectric constants are equal; this will be assumed to be the case in the present treatment. After an integration of (1) which can be readily carried out because the currents in the blocking static case are zero,[1] we obtain, on using the Einstein relation between D_n and μ_n

$$dn/dx = -(e/kT)En. \quad (7)$$

Equation (3) becomes[4]

$$k_2 np = k_1(N-p), \quad (8)$$

where N is the homogeneous concentration of neutral centers before any dissociation is assumed to have occurred. The concentration of neutral centers in a region where the concentration of fixed positive centers is $p(x)$ must be simply $(N-p)$ as in (8) since the positive charge concentration p is assumed to arise entirely by dissociation from neutral centers.

Before solution of the above equations, it will be helpful to normalize the quantities of interest. Define the Debye length for a concentration N of charges of one sign mobile as $L_{D_1}=[\epsilon kT/4\pi e^2 N]^{\frac{1}{2}}$. This is the minimum Debye length and arises when all neutral centers are ionized. When there is incomplete ionization and nonzero recombination, the effective Debye length, L_e, will be greater, since the concentration of mobile charge is then decreased. Let $L_e \equiv \theta L_{D_1}$, where the correction factor θ will be determined later. Let

$$\psi^* = \psi/(kT/e); \qquad n^* \equiv n/N; \qquad p^* \equiv p/N;$$

$$E^* \equiv E/(kT/eL_e); \qquad R \equiv k_2 N/k_1;$$

$$z \equiv x/L_{D_1}; \quad \text{and} \quad x^* = x/L_e.$$

The quantity z is a measure of distance in terms of the number of fixed minimum Debye lengths, while x^* measures the number of effective Debye lengths, the quantity of greater interest. Note that the recombination ratio R depends only on material properties. When R is zero, there is no recombination.

Written in terms of normalized variables, the pertinent equations become

$$dn^*/dx^* = -E^* \cdot n^*, \quad (7')$$

$$dE^*/dx^* = \theta^2(p^*-n^*); \quad (4')$$

$$E^* = -d\psi^*/dx^*, \quad (5')$$

$$p^* = [1+Rn^*]^{-1}. \quad (8')$$

Equations (6) are automatically satisfied since there is no current at the blocking electrode or elsewhere.

The above set of equations can be partly solved by

† A glossary of symbols appears at the end of this paper.

[14] S. M. Skinner, J. Appl. Phys. **26**, 498 (1955).

[15] D. C. Grahame, Chem. Revs. **41**, 441 (1947).

[16] J. R. Macdonald, J. Chem. Phys. **22**, 1857 (1954).

substituting (8′) in (4′), differentiating (7′) with respect to x^*, and eliminating E^* and dE^*/dx^* from the resulting equation using (4′) and (7′). The resulting second-order nonlinear differential equation in n^* can be transformed to a linear Bernoulli equation, then integrated directly. The result is

$$[(1/n^*)(dn^*/dx^*)]^2 = A + 2\theta^2 n^* + 2\theta^2 \ln\{(1+Rn^*)/n^*\}. \quad (9)$$

On using (7′), this equation may be written

$$(E^*)^2 = A + 2\theta^2\{n^* + \ln[(1+Rn^*)/n^*]\}, \quad (9')$$

where A is an integration constant. By combining Eqs. (7′) and (5′), one can obtain

$$(1/n^*)(dn^*/dx^*) = -E^* = d\psi^*/dx^*. \quad (10)$$

Let us fix the zero of potential at $x^* = \infty$ and define n^*_∞ as the value of n^* there. Integration of (10) then yields

$$n^* = n^*_\infty e^{\psi^*}. \quad (11)$$

At $x^* = \infty$, n^* and p^* are equal and E^* is zero. Equation (8′) therefore leads to the relation

$$n^*_\infty = -(1/2R) + [(1/2R)^2 + (1/R)]^{\frac{1}{2}}, \quad (12)$$

a reasonably well-known equation.[4,17] Thus, n^*_∞ is the common, normalized value of the mobile and fixed charge concentrations in the absence of space charge; it is unity for $R=0$ and equal to $R^{-\frac{1}{2}}$ for very large R.

Using the boundary condition at $x^* = \infty$, the integration constant A in (9′) may be evaluated. On introducing (11) as well, one finds

$$E^*(\psi^*) = -(d\psi^*/dx^*) = \pm\sqrt{2}\theta[n^*_\infty(e^{\psi^*}-1) + \ln\{(e^{-\psi^*}+Rn^*_\infty)/(1+Rn^*_\infty)\}], \quad (13)$$

where the sign of E^* is selected such that it is directed from positive to negative charges. Equation (13) may also be written as follows, using $n^*_\infty = (1+Rn^*_\infty)^{-1}$,

$$E^*(\psi^*) = \pm\sqrt{2}\theta[n^*_\infty(e^{\psi^*}-1) + \ln\{1+n^*_\infty(e^{-\psi^*}-1)\}]^{\frac{1}{2}}. \quad (13')$$

At $x=0$, $\psi=\psi_0$, the externally applied potential plus any contact or surface potential at the boundary. Thus, the normalized field at the blocking electrode is obtained by replacing ψ^* by ψ^*_0 in (13′). Note that ψ^*_0 may be either positive or negative. The formal solution to the present problem is given by rewriting (13) or (13′) as an integral,

$$x^* = \frac{\mp 1}{\sqrt{2}\theta}\int_{\psi^*}^{\psi^*_0} \frac{d\psi^*}{[n^*_\infty(e^{\psi^*}-1) + \ln\{1+n^*_\infty(e^{-\psi^*}-1)\}]^{\frac{1}{2}}}, \quad (14)$$

which specifies how ψ^* and x^* are connected for given values of ψ^*_0 and n^*_∞. The $\mp$ sign is chosen so that x^* is positive whatever the sign of ψ_0^* and ψ^*.

Although (14) cannot be integrated exactly in closed form, it may be evaluated to any desired accuracy by digital computer quadrature. Further, it can be integrated in certain limiting cases to yield approximate but explicit relations between ψ^* and x^*. When $n^*_\infty(e^{-\psi^*}-1) \ll 1$, (14) becomes

$$x^* = 1/\sqrt{2}\int_{\psi^*}^{\psi^*_0}\{d\psi^*/[\cosh\psi^* - 1]^{\frac{1}{2}}\} = \ln\{\tanh(\psi^*_0/4)/\tanh(\psi^*/4)\}, \quad (15)$$

the known solution of the one-blocking-electrode problem when changes of both sign are mobile and recombination is zero.[1] In that case x^* is normalized with $L_e = L_{D_2} = L_{D_1}/\sqrt{2}$, however. In the present case, when R is large the fixed charges are effectively mobilized and the effective Debye length $L_e \equiv \theta L_{D_1}$, becomes $[\epsilon kT/8\pi e^2 n_\infty]^{\frac{1}{2}}$ equal to L_{D_2} except that N is replaced by n_∞. Thus, this approximate solution then differs from the corresponding two-mobile case only in the difference between n_∞ and N. In particular, the dependence of ψ^* on x^* will be exactly the same for $\sqrt{R} \gg 1$.

Another case of interest is that where ψ^* is large and negative so that $n^*_\infty e^{|\psi^*_a|} \gg 1$. Equation (14) then becomes

$$x^* \cong \frac{-1}{\sqrt{2}\theta}\int_{-\psi^*}^{-\psi^*_0} \frac{d\psi^*}{[-\psi^* - n^*_\infty + \ln n^*_\infty]^{\frac{1}{2}}} = (\sqrt{2}/\theta)\{[|\psi^*_0| - n^*_\infty + \ln n^*_\infty]^{\frac{1}{2}} - [|\psi^*| - n^*_\infty + \ln n^*_\infty]^{\frac{1}{2}}\}. \quad (16)$$

This result applies of course only when $\psi^*_0 \ll -1$ and $|\psi^*| > (n^*_\infty - \ln n^*_\infty)$. It is useful, however, in delineating most of the exhaustion and depletion region that forms in the neighborhood of the blocking electrode when ψ^*_0 is large and negative and the mobile charges are negative as well, as in the present case. Had we taken the mobile charges positive instead of negative, the present case would have arisen on the application of a large positive potential.

Next, consider the case $\exp(\psi^*) \gg 1$. Then (14) becomes approximately

$$x^* \cong \frac{1}{\sqrt{2}\theta}\int_{\psi^*}^{\psi^*_0} \frac{d\psi^*}{[n^*_\infty \exp\psi^*]^{\frac{1}{2}}} = [2/\theta(2n^*_\infty)^{\frac{1}{2}}][\exp(-\psi^*/2) - \exp(-\psi^*_0/2)]. \quad (17)$$

On solving for ψ^* in terms of x^*, one finds

$$\psi^* \cong 2\ln\{\exp(-\psi^*_0/2) + (n^*_\infty\theta^2/2)^{\frac{1}{2}} \cdot x^*\}^{-1}. \quad (17')$$

This expression shows how ψ^* depends on x^* in the immediate neighborhood of the blocking electrode when ψ^*_0 is of the proper sign and of sufficient magni-

[17] N. L. Pisarenko, Izvest. Akad. Nauk S.S.S.R. Ser. Fiz. 3, 631 (1938).

tude to produce an appreciable charge accumulation region near the electrode. For large R, $(n^*_\infty\theta^2/2)^{\frac{1}{2}}$ approaches $\frac{1}{2}$. Formula (17) is then of exactly the form obtained in the analogous two-mobile case, except again N in the L_{D_2} for the two-mobile case is here replaced by n_∞.

The $R=0$ case for $|\psi^*|\ll 1$ requires special treatment. Equation (14) becomes, noting that $n^*_\infty=1$ and $\theta=1$,

$$x^*\cong\frac{1}{\sqrt{2}}\int_{\psi^*}^{\psi^*_0}\frac{d\psi^*}{[\exp(\psi^*)-1-\psi^*]^{\frac{1}{2}}}\cong\int_{\psi^*}^{\psi^*_0}\frac{d\psi^*}{\psi^*}$$
$$=\ln(\psi^*_0/\psi^*). \quad (18)$$

Thus,

$$\psi^*\cong\psi^*_0(\exp-x^*). \quad (18')$$

Note that an equation similar to (18′) is also obtained from (15) when $(\psi^*_0/4)\ll 1$.

Equations (15), (16), (17), and (18), although approximate, should usually suffice to allow most of the space-charge regions of interest to be calculated with sufficient accuracy for comparison with experiment. Experimental measurement of potential distributions can be made for distances as small as 2×10^{-3} cm by moving a sharp probe along the surface of the material[18] and using a vibrating reed electrometer, but certain precautions must be observed. It is desirable that any contact, surface, or floating potential between the probe and the surface be eliminated or reduced by making the contact nonrectifying.[19] The probe will then measure the average lattice potential at its position. A possible method of making effectively ohmic contacts to insulating crystals such as CdS has been described by Smith.[20] In practice, various probe materials and surface treatments may often be used to reduce floating potentials to a level considerably below that of the desired space-charge potential. It should be pointed out that since ψ_0 and ψ have been defined to include the contributions of any surface or contact potentials at the blocking electrode, measurements with a potential probe and electrometer will only yield that part of the internal potential difference arising from the applied potential, not including blocking-electrode contact potentials. We have elected to include such potentials in ψ, however, when they exist, since they can still lead to space charge in the neighborhood of the electrode and their presence can be inferred from capacitance measurements, as discussed later.

DISCUSSION OF STATIC DISTRIBUTION CURVES

Figures 1 through 6 illustrate space-charge behavior for various conditions. The curves of these figures have been calculated from Eq. (14) using an IBM 650 computer.[21] Although we only show the dependence of ψ^* on normalized distance, that of n^*, p^*, and E^* can be obtained using the ψ^* results and Eqs. (11), (12), (8′), and (13′), together with the expression for θ given in the next section.

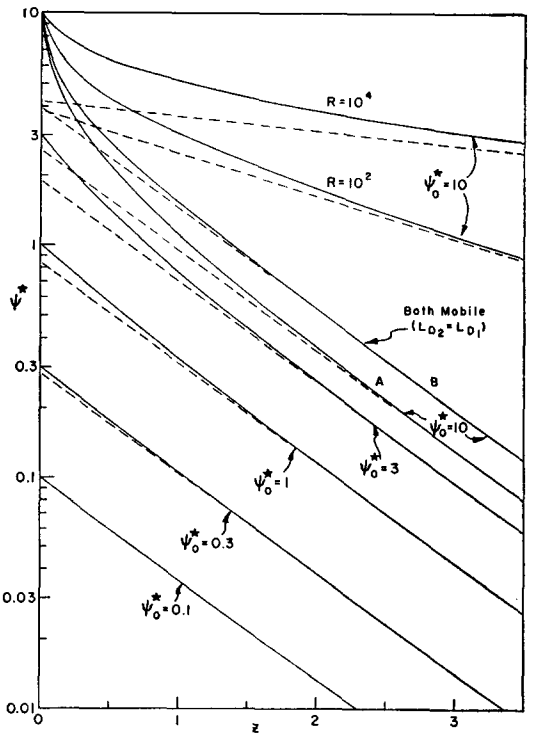

FIG. 1. Accumulation-region potential curves for various values of applied normalized potential *versus* normalized distance. The six lower curves are for $R=0$.

Figure 1 illustrates the development of a charge accumulation region as the applied normalized potential is increased from very small values. In this figure, all but the top two curves are for $R=0$. Note that the curve for $\psi^*_0=0.1$ is well fitted by Eq. (18′) but that the other curves progressively deviate from exponential behavior in the small z region as ψ^*_0 increases.

The two top curves show how the space-charge region is spread out for nonzero recombination. Since the abscissa is here z, the normalization of distance is constant independent of R. Were the top two curves replotted *versus* x^* so that comparison could be made on the basis of an equal number of effective Debye lengths (depending on R through θ), both top curves would fall between the curves marked A and B in the figure. For $R=10^8$, the resulting curve is indistinguishable from B, that for the case where both positive and negative charges are mobile. The condition for applicability of Eq. (15) is well satisfied in this case. Since

[18] Pearson, Read, and Shockley, Phys. Rev. **85**, 1055L (1952).
[19] H. K. Henisch, *Rectifying Semi-Conductor Contacts* (Oxford University Press, London, 1957), pp. 274–275.
[20] R. W. Smith, Phys. Rev. **97**, 1525 (1955).
[21] Copies of this program for IBM 650 computer use are available to any who may require more accurate solutions than those given by the approximate results of Eqs. (15), (16), (17), and (18).

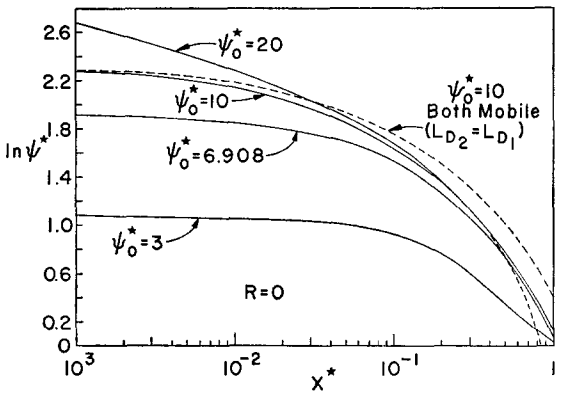

FIG. 2. Log-log plot of accumulation region normalized potential in the neighborhood of the blocking electrode *versus* normalized distance. The dotted line at the right is calculated from an approximate expression.

curves for all R values fall in the narrow region between A and B, we see that on comparing in terms of effective Debye lengths, R has very little effect on the space-charge distribution in the accumulation case.

When ψ^*_0 is greater than about 10 (equivalent to approximately 0.25 volt at room temperature), the accumulation layer builds up only in the region of very small z and the rest of the curve remains the same as that for $\psi^*_0=10$. This effect is illustrated by the log-log curves of Fig. 2. For $x^*>0.2$, the $\psi^*_0=20$ and $\psi^*_0=10$ curves are indistinguishable. The dotted curve at the right of the figure illustrates how the approximation (17′) deviates from the correct result for $x^*>0.4$. Note that the x^* and z scales are identical in the $R=0$ case.

We have not illustrated accumulation layers for $\psi^*_0>20$ for two reasons. First, for small R, they lead to exceptionally high fields and charge concentrations at $x=0$.[3] Experimentally, high-field emission, dielectric saturation, etc., will occur before such fields and concentrations are reached. For $R=0$, $\psi^*_0=20$ leads to a normalized field $E^*_0=3.12\times10^4$ at $x^*=0$. At room temperature, this corresponds to an actual field of 8×10^6 volts/cm for an effective Debye length of 10^{-4} cm. It may also be pointed out that high fields may have an effect on recombination and emission[22] and that the concept of electron motion in a conduction band is itself not useful if the field is very high.[23] Finally, it should be mentioned that for high ψ^*_0 the mathematics may call for not only exceptionally high charge concentrations at the electrode but extremely rapid decrease in the concentration as z increases from zero. It is clear that the physical situation will not conform to the mathematical solution if the mean free path of the mobile charges is greater than the distance in which ψ^* and n^* are required to change appreciably. In this case, the terms which describe diffusion in the equations will certainly be inapplicable.

When R is very great, the situation is somewhat different. The large value of R produces a small value of n^*_∞, and the field and charge concentration at the blocking electrode will not necessarily be excessive. In terms of x^*, the decay of ψ^* away from the electrode will still be very rapid but L_e may be so large that the decay will actually take place over appreciable distances. As an example, consider the case $R=10^{40}$, $\psi^*_0=50$. Then $n^*_\infty=10^{-20}$. If $N=10^{18}$ cm^{-3}, for example, the material is essentially insulating. The quantity θ is $10^{10}/\sqrt{2}$ and even for an L_{D_1} of 10^{-7} cm, L_e is 7×10^2 cm. For this same L_{D_1}, the field at the electrode is 2.6×10^6 volts/cm. The normalized potential drops from 50 to 20 in 6.4×10^{-2} cm and to 10 in 32 cm. At the latter point, n^* is 2.2×10^{-16}. Because of the very few free carriers present in material with such a high recombination ratio, it will be difficult to measure the dependence of potential on distance from the blocking electrode even though the distance scale is favorable.

Figure 3 illustrates the progressive formation of a depletion and exhaustion region at the blocking electrode when fields are present which draw the mobile charge away from the electrode. The dotted line on the $\psi^*_0=-10$ curve is calculated from Eq. (16); for $|\psi^*|>2$, this equation fits the curves of the figure extremely well. The mathematical solution calls for extremely small but nonzero n^* values when $\psi^*\ll-1$. For example at $\psi^*=-100$ and $R=0$, $n^*\simeq4\times10^{-44}$. This value is completely negligible and can be replaced

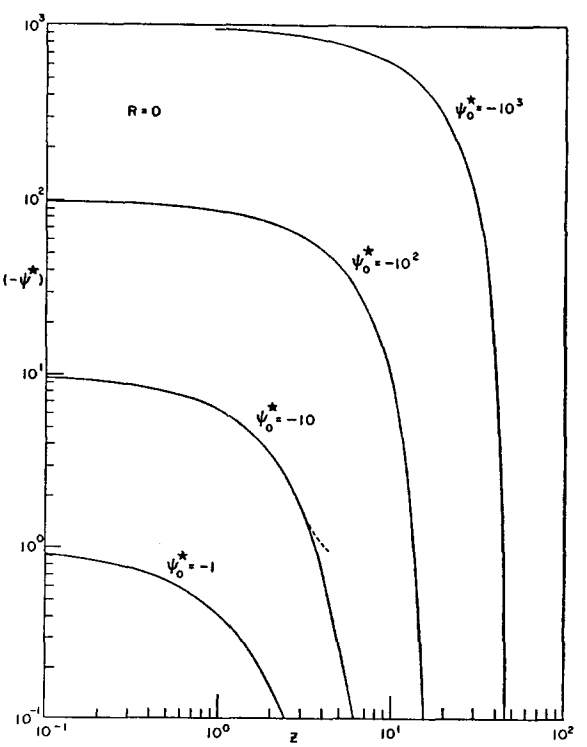

FIG. 3. Exhaustion-depletion region potential-distance curves for various values of applied normalized potential. The dotted line represents an approximate expression.

[22] F. G. Bass, Zhur. Eksptl. i Teoret. Fiz. **32**, 863 (1957).
[23] E. N. Adams, Phys. Rev. **107**, 698 (1957).

by zero with no effect on the potential distribution. Because n^* is so small in the exhaustion region, recombination has little effect on the curves in this region using the z scale. Thus, for $\psi^*_0=-1000$, $z=37.10$ at $\psi^*=-30$ for $R=0$ and is 39.52 at $\psi^*=-30$ for $R=10^{16}$.

The present treatment is based on the assumption of a continuous space charge. For it to apply, it is necessary that the exhaustion region thickness be large compared to the average distance between ionized centers, $N^{-\frac{1}{3}}$ cm. From (16) the approximate exhaustion layer thickness ($|\psi^*_0| \gg |-\ln n^*_\infty + n^*_\infty|$) is

$$L_{D_1}(2|\psi^*_0|)^{\frac{1}{2}}=[\epsilon|\psi_0|/2\pi eN]^{\frac{1}{2}}$$

Thus, the exhaustion layer solution is only a good approximation when this quantity is at least five or ten times greater than $N^{-\frac{1}{3}}$. Taking the factor as 10, we obtain the condition for validity, $|\psi_0| \geq 200\pi eN^{\frac{1}{3}}/\epsilon$.

The strong exhaustion regions illustrated in Fig. 3 are very similar to those found with reversed-biased *pn* junctions, as discussed in the next sections. Mathematically, the mobile charge concentration in the exhaustion region follows the Maxwell-Boltzmann distribution of Eq. (11) and reaches extremely small values. Physically, it will actually be zero over most of the region. In the region of very low concentration, the diffusion terms in the equations will not be applicable and the field will withdraw all mobile charge

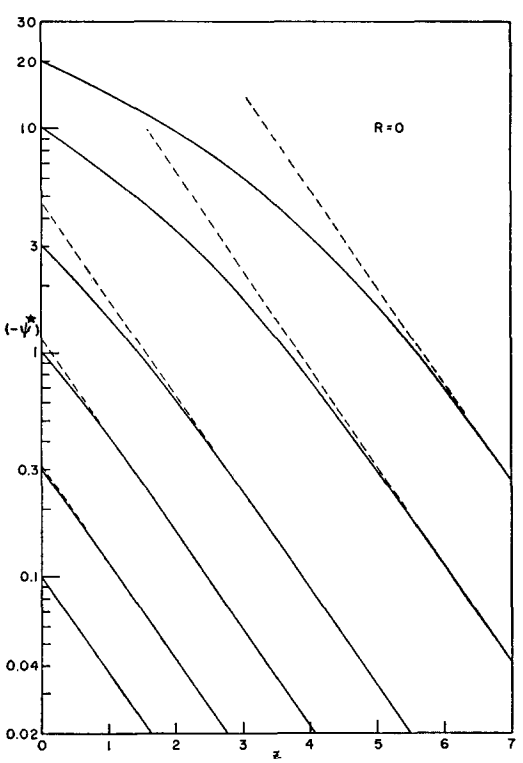

FIG. 4. Potential-distance curves showing the initial formation of a depletion-exhaustion region for low applied normalized potentials.

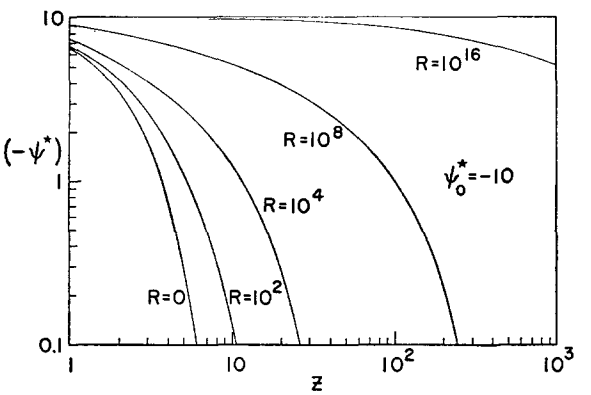

FIG. 5. Exhaustion region potential-distance curves for $\psi_0^*=-10$ and various values of the recombination ratio, R. Distance scale normalization independent of R.

from most of the exhaustion region. Consider a charge near the boundary of the exhaustion region where the charge concentration is appreciable. In the statistically unlikely event that almost all the available thermal energy of the material should be transferred to this one charge at a certain instant (and the rest of the material thereby cooled to almost absolute zero), the charge might start off toward the blocking electrode against the influence of the internal field. Like a ball thrown upward, it would penetrate only so far into the exhaustion region and would then return. Thus, for appreciable potential drop across the depletion-exhaustion region, it must be at least partly depleted entirely of mobile charge.

Figure 4 illustrates the initial setting up of a depletion region starting from very small ψ^*_0. These curves should be compared with the corresponding ones of Fig. 1 for the buildup of accumulation regions. Equation (18′) is again applicable for very small ψ^*. Figure 5 shows the effect of recombination for $\psi^*_0=-10$, not so negative a value that n^* is negligible in the depletion region. Using the z scale, R appears to make a very appreciable difference in the curves. Comparing on the basis of number of effective Debye lengths, as in Fig. 6, however, we see that the difference is not very great. The latter is the more reasonable mode of comparison. It will be noted that as R increases, the potential distribution gradually changes from that of an exhaustion region to that of an accumulation region in the neighborhood of the blocking electrode. The final $R\geq 10^8$ curve is exactly the same as that for the two-mobile case in Fig. 1 and is described by Eq. (15). As recombination increases, the fixed positive charges become essentially mobile through recombination and an excess of them (but $\leq N$) buildup near the blocking electrode while a deficit of negative charge is formed there. For $R\geq 10^8$, the concentrations of positive and negative charge are almost exactly reversed in the neighborhood of the electrode for $\psi^*_0=\pm 10$. Such reversal can only occur exactly when the maximum

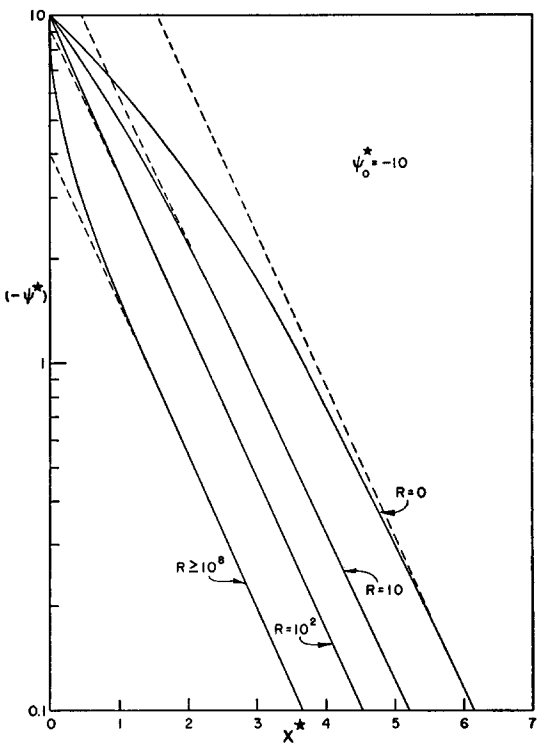

FIG. 6. Exhaustion region potential-distance curves for $\psi_0^* = -10$ and various values of R. Distance scale measures number of effective Debye lengths and normalization is therefore a function of R.

value of n^* does not exceed unity since p^* can never exceed this value. For very negative applied potentials such as $\psi^*_0 = -50$, it requires values of R such as 10^{50} to cause this condition to be met. In general, for $n^*_{max} = n^*_\infty \exp(\psi^*_0) \leq 1$ to hold, it is necessary that $\exp(\psi^*_0) \leq R^{\frac{1}{2}}$, for large R. For a depletion layer to turn to an accumulation layer, the same condition with the absolute value of $|\psi^*_0|$ taken applies. Since $\psi^*_0 = -1000$ corresponds to only about -25 volts at room temperature, the maximum value of R found experimentally will usually not be great enough for the above condition to hold for most applied potentials.

Various conditions under which the mathematical solution does not correspond to a physically realizable situation have already been noted. It should additionally be pointed out that since the present solution is one-dimensional, edge and surface effects are neglected. There will be situations where surface recombination and surface states will exert appreciable influence on static space-charge distributions but they are outside the scope of the present one-dimensional treatment.

The present treatment is also implicitly limited to Maxwell-Boltzmann statistics. In samples where electrons or holes are the mobile carriers, the present solution will not be accurately applicable when mobile charge concentrations reach degeneracy, and Fermi-Dirac statistics must be used. Two cases may be mentioned. When n_∞ is in the degenerate region, the Einstein-Boltzmann relation between μ and D will not hold but must be replaced, e.g., in (7), and in the expression for L_{D_1} by a relation involving integrals over the Fermi-Dirac distribution function. This greatly complicates solution of the equations. Secondly, in an accumulation region, n may be large enough for degeneracy even though n_∞ is not. In this case, the electric field will generally be large enough in this region (provided breakdown or saturation has not occurred) that band theory will not be applicable[23] and the values of $n(x)$ will depart from the predictions of the present solution.

In some experimental situations, the blocking electrode may not be completely blocking but may allow a small leakage current to flow on the application of a potential difference to the material. Additionally, in semiconductors intrinsic generation of mobile holes and electrons will contribute charges not considered in the present theory. These sources of additional charge will usually not alter the charge distribution appreciably in the regions where the normal space-charge concentration is high. They may determine the minimum charge concentrations in exhaustion regions, but are not likely to alter the potential distributions appreciably. As long as the additional charge is small, the fields of the present treatment may be considered as acting on the additional charge without themselves being much changed by it.

In the present treatment, the impurity concentration N has been assumed homogeneous. Were there any experimental reason to expect it to vary appreciably with position, such variation could be readily incorporated into the space-charge equations and a digital computer solution produced with little more difficulty than in the present case.

Finally, the present solution has been applied to a sample of semi-infinite length. As the foregoing curves show, the actual length necessary for the internal potential have decayed in magnitude by a factor of ten or more from its value at the blocking electrode is no more than three effective Debye lengths for an accumulation region and approximately [from Eq. (16)] $(2|\psi^*_0|)^{\frac{1}{2}} L_{D_1}$ lengths for an exhaustion region. If an ohmic contact is placed along the specimen a distance equal or greater to those above instead of at $x = \infty$, the actual space-charge distribution in the portion of the sample between the blocking and ohmic contacts will be little altered. The potential distribution need not be altered at all for even shorter lengths provided the added electrode is not exactly ohmic. All that is necessary is to add an electrode at whatever the desired distance that will ensure duplication of the infinite-length-solution field, potential, and charge concentrations at the point of addition. Such an electrode will not be ohmic since it will have a potential drop across it equal to the potential difference from the point of addition to $x^* = \infty$ in the infinite-length

solution. The more usual case where both electrodes are completely blocking will be discussed in a succeeding paper.

CHARGE AND CAPACITANCE

When an exhaustion or accumulation region forms, the total charge in the system is less or greater than that before an external potential is applied because of transient mobile charge flow through the ohmic electrode. The changes in the positive and negative charges may be written

$$q_p = e\int_0^\infty [p(x) - p_\infty]dx = eNL_e\int_0^\infty [p^*(x^*) - p^*_\infty]dx^*, \tag{19}$$

$$q_n = e\int_0^\infty [n(x) - n_\infty]dx = eNL_e\int_0^\infty [n^*(x^*) - n^*_\infty]dx^*; \tag{20}$$

these are really charges per unit cross-sectional area, but for convenience we shall omit further mention of this fact in speaking of charges and capacitance in the rest of this section. The negative charge on the blocking electrode is from Gauss's law, just

$$q_0 = q_n - q_p = (-\epsilon/4\pi)\, E_0 = (kT/e)\,(\epsilon/4\pi L_e)[-E^*_0], \tag{21}$$

where E_0 is the electric field immediately at the blocking electrode. Noting that $eNL_e = (\epsilon kT\theta^2/4\pi eL_e)$ and using (5), (19) and (20) become

$$q_p = (kT/e)\,(\epsilon\theta^2/4\pi L_e)\int_0^{\psi^*_0} \frac{[p^*(\psi^*) - p^*_\infty]d\psi^*}{|\,E^*(\psi^*)\,|},$$

$$= (kT/e)\,(\epsilon/4\pi L_{D_2})[\exp(-\psi^*_0/2) - 1]$$

(two-mobile case); (19′)

$$q_n = (kT/e)\,(\epsilon\theta^2/4\pi L_e)\int_0^{\psi^*_0} \frac{[n^*(\psi^*) - n^*_\infty]d\psi^*}{|\,E^*(\psi^*)\,|}$$

$$= (kT/e)\,(\epsilon/4\pi L_{D_2})[\exp(\psi^*_0/2) - 1]$$

(two-mobile case). (20′)

For the present one-mobile case, (19′) and (20′) may be written more explicitly by substitution of Eqs. (8′), (11), (12), and (13′). They may then be integrated using a digital computer or other method. When these equations are combined as in (21) to give q_0, it may readily be shown that q_0 may be expressed as in the right-hand side of (21) without the need for integration. The $\pm$ sign in E^* is selected to that q_0 is positive for ψ^*_0 positive and negative when it is negative. Here e is the arithmetic charge and q_0 is an unsigned charge magnitude; if e includes the sign of the charge, q_0 will be negative, representing an excess of negative charge when ψ^*_0 is positive. Note that $E^*(\psi^*_0) \equiv E^*_0$ can be obtained from (13′) with ψ^* set equal to ψ^*_0. Since q_0 is a quantity which is readily measurable, it is convenient that it can be obtained without integration.

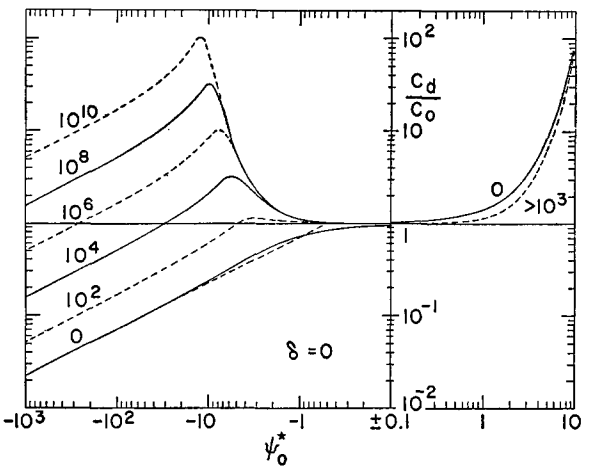

FIG. 7. Normalized differential capacitance *versus* positive and negative applied normalized potential for various R values.

The static and differential capacitances may now be written

$$C_s = |\,q_0/\psi_0\,| = (\epsilon/4\pi L_e)\,|\,E^*_0/\psi^*_0\,|, \tag{22}$$

$$C_d = |\,dq_0/d\psi_0\,| = (\epsilon/4\pi L_e)\,|\,dE^*_0/d\psi^*_0\,|$$

$$= (\epsilon\theta^2/4\pi L_e)\,|\,(n^*_0 - p^*_0)/E^*_0\,|, \tag{23}$$

where n_0 and p_0 are the values of n and p at $x=0$ and $\psi^* = \psi^*_0$, and the relation $1 - n^*_\infty = Rn^{*2}_\infty$ has been used in simplifying (23). For the two-mobile case, C_s and C_d have already been given as explicit functions of ψ^*_0 elsewhere.[3]

We are now in a position to determine the quantity θ. Let $C_0 = \epsilon/4\pi L_e$, the common value of C_s and C_d as $\psi^*_0 \to 0$. If now we carry out the limit $\psi^*_0 \to 0$ in either (22) or (23), C_s/C_0 and C_d/C_0 should approach unity. Since these equations involve θ, it is therefore determined. The result is

$$\theta = [n^*_\infty(1 + Rn^*_\infty)]^{-\frac{1}{2}} = [n^*_\infty(2 - n^*_\infty)]^{-\frac{1}{2}}. \tag{24}$$

The effective Debye length may now be written as

$$L_e = \theta L_{D_1} = [\epsilon kT/4\pi e^2 Nn^*_\infty(2 - n^*_\infty)]^{\frac{1}{2}}. \tag{25}$$

When R is large and recombination important, $n^*_\infty \ll 2$. Since $Nn^*_\infty = n_\infty$, L_e will then approach the two-mobile Debye length, L_{D_1} with N replaced by n_∞, as stated earlier. In this case, the positive carriers are effectively mobilized by recombination.

Figure 7 shows how the normalized differential capacitance depends on potential for various recombination ratio values. Note that the potential increases negatively to the left. For positive ψ^*_0, the accumulation layer has a capacitance which increases as $\exp(\psi^*_0/2)$ for large ψ^*_0. For $R > 10^3$, the resulting curve is that also obtained in the two-mobile case.[3] Note that C_0 will decrease as R increases. For $R = 0$

and $\psi^*_0<0$, an exhaustion region is formed and the capacitance eventually decreases proportional to $\psi^{*-\frac{1}{2}}_0$ as in an abrupt pn junction.[24]

When $\psi^*_0<0$ and $R>0$, the situation is somewhat different. The C_d/C_0 curve for appreciable R is initially a mirror image of that obtained for $\psi^*_0>0$ but eventually reaches a maximum then decreases, reaching a final slope equal to that of the $R=0$ case. What is happening is that the negative potential draws mobile charge away from the neighborhood of the electrode. This reduction of n^* leads to a corresponding increase in p^* (initially much less than unity for $R\gg1$) through recombination-dissociation. This increase continues and an accumulation region is formed until almost all mobile charge is removed from the electrode region at $x^*=0$. Then p^* is nearly equal to unity, its maximum value. Further increase in negative potential soon causes a depletion-exhaustion region to form and the capacitance begins to decrease. For $R>10^3$, the maximum value of C_d/C_0, which occurs at $(-\psi^*_0)\simeq1+\ln R^{\frac{1}{2}}$, is given quite closely by $R^{\frac{1}{2}}/10^{\frac{1}{2}}$.

From either a detailed comparison of experimental and theoretical C_d/C_0 curves of the present form or from the maximum value of C_d/C_0 alone, it should be possible to calculate R quite accurately. Then n^*_∞ and θ can be calculated. Next, from knowledge of ϵ and θ and the measured value of C_0, L_e and N may be obtained. Finally, n_∞ and k_2/k_1 may be calculated. Knowledge of L_e is necessary in comparing theoretical and experimental potential distribution curves. Further, the present measurement methods are readily applicable to studies of the dependence of n_∞ and k_2/k_1 on temperature or light intensity for thermal or optical activation, respectively.

The static capacitance curves, C_s/C_0, are similar to those shown in Fig. 7, but for $\psi^*_0<0$ and $R\gg1$ the peaks are not as high as those of C_d/C_0 and occur at somewhat more negative potentials. It should be mentioned that the measurement of C_d should be made at a sufficiently low frequency that a period of the measuring frequency is long compared to the recombination-dissociation time. Since this time will generally be very short, audio-frequency measurements will usually be adequate. Clearly, if measurements can be extended to sufficiently high frequencies that this condition will not hold, useful information concerning recombination time can be obtained.

BLOCKING LAYER EFFECTS

The preceding capacitance results implicitly assume that an electrode can be attached to the material under investigation which will be blocking and yet will have no potential drop between it and the material except possibly a contact or surface potential ϕ_0 which is usually taken independent of any external applied potential. This situation will often be difficult to achieve; instead there may be an additional potential drop between the metallic electrode and the space-charge region we have heretofore been considering. To achieve an electrode which is blocking for either entry or withdrawal of the mobile carriers or both, it will often be necessary to have next to the electrode a region of either basic material or of extraneous material which has a very low concentration of fixed and mobile charges. In the first case, the intermediate region is called a natural blocking layer; in the second, an artificial blocking layer. For example, to achieve complete blocking of mobile electrons, a layer could be used of an insulator such as mica taken sufficiently thick that tunneling or dielectric breakdown would not occur. When the mobile carriers are ions or vacancies, a separate blocking layer will usually not be required to achieve adequate blocking at the electrode over an appreciable range of applied potentials.

When an additional layer of the above form is present, part of the applied potential, now denoted ψ_a, will distribute itself across this layer, while the remaining part, ψ_0, will appear across the space-charge region. In accordance with the above assumptions, the blocking layer will have a potential-independent capacitance C_{ser}. Those cases where the capacitance of this layer may be potential dependent because of electrostriction or dielectric saturation[16] are outside the scope of the present treatment. We shall also neglect the very rapid decrease towards zero of mobile charge in the charge-free layer at its boundary with the space-charge region and assume that the charge-free region is actually entirely charge free. The capacitance C_{ser} and that of the space-charge layer, C_d or C_s, are in series, and since the space-charge capacitance is potential dependent, the actual potential division between C_{ser} and C_s will depend on ψ_a. Let $C_0/C_{ser}=\delta$, a quantity independent of ψ_a. The conditions of field and potential continuity at the interface between the main homogenous material and the blocking layer require that the charge on the capacitor C_s be equal to the distributed space charge, e.g., q_0. The series blocking-layer capacitor is formed by the metal electrode, the (essentially) insulating blocking layer, and the space-charge region acting as the other electrode. The condition of charge equality yields

$$C_{ser}(\psi_a-\psi_0)=q_0=C_s\psi_0, \tag{26}$$

or

$$\psi^*_a-\psi^*_0=(C_0/C_{ser})\,(C_s/C_0)\psi^*_0=\delta\cdot\psi^*_0\cdot(C_s/C_0). \tag{26'}$$

Since C_s/C_0 is itself a function of ψ^*_0, Eq. (26') is a transcendental equation for ψ^*_0 when ψ^*_a is given. Alternatively, a value of ψ^*_0 can be assumed and the corresponding value of ψ^*_a calculated directly from (26') using (22) for C_s.

The quantities actually accessible to measurement are the series combinations of C_{ser} and C_s or C_d. The

[24] W. Shockley, Bell System Tech. J. **28**, 435 (1949).

differential capacitance of the series combination of C_{ser} and C_d, C_c, which is generally the quantity of most interest, is given by

$$C_c = C_{ser}[\delta(C_d/C_0)]/[1+\delta(C_d/C_0)]$$
$$= C_{c0}[(1+\delta)(C_d/C_0)]/[1+\delta(C_d/C_0)], \qquad (27)$$

where C_{c0}, the zero-potential value of C_c, is $C_{ser}\delta/(1+\delta)$. Note that when $\delta C_d/C_0 \gg 1$, that is, $C_d \gg C_{ser}$, C_c is essentially just C_{ser} as it should be. A procedure for determining the dependence of C_c on δ, R, and ψ^*_a is as follows. First, the relation between a ψ^*_0 value and the corresponding ψ^*_a value is determined from (26′). Then (27) is used to calculate C_c. Since this procedure is fairly complex, it has been programed for IBM 650 calculation.[25]

Before discussing the results of such calculations, it is of interest to compare the present treatment with previous approaches. First, the Mott barrier[26,27] assumes a charge-free region between the electrode and the body of the material. As in the present case, the field is taken as constant in this region and the potential distribution is linear. However, no space charge is assumed abutting the blocking layer, and the capacitance of the system is a constant essentially independent of applied potential. In Schottky's theory of barrier-layer rectifiers,[28,29] a space-charge region produced by fixed, completely ionized charges is taken into account but no charge-free layer is considered and recombination between fixed and mobile charges is neglected. In addition, the space charge arising from mobile carriers, an important feature of the present treatment, is assumed to be of negligible importance in the Schottky theory. Finally, Billig and Landsberg[30] have combined the assumptions of the Mott and Schottky theories in such a way that it is possible to pass continuously from one to the other. In the resulting combined theory, the capacitances of the insulating layer and the space-charge layer combine reciprocally in the usual fashion of capacitances in series, but the neglect of the effects of mobile carriers allows a transcendental equation such as (32) to be avoided and the over-all capacitance to be expressed as an explicit function of the total applied potential. Because of this approximation, the distribution of potential drop across the charge-free and the space-charge regions will differ between the present case and that of Billig and Landsberg. Note that in most of these treatments, including the present work, the effects of tunneling and image forces have been assumed negligible.

[25] Copies of this program are also available.
[26] N. F. Mott, Proc. Roy. Soc. (London) **A171**, 27, 144 (1939).
[27] See reference 19, pp. 191–192.
[28] W. Schottky and E. Spenke, Wiss. Veröffentl Siemens-Werken **18**, 225 (1939).
[29] W. Schottky, Z. Physik **118**, 539 (1942).
[30] E. Billig and P. T. Landsberg, Proc. Phys. Soc. (London) **A63**, 101 (1950).

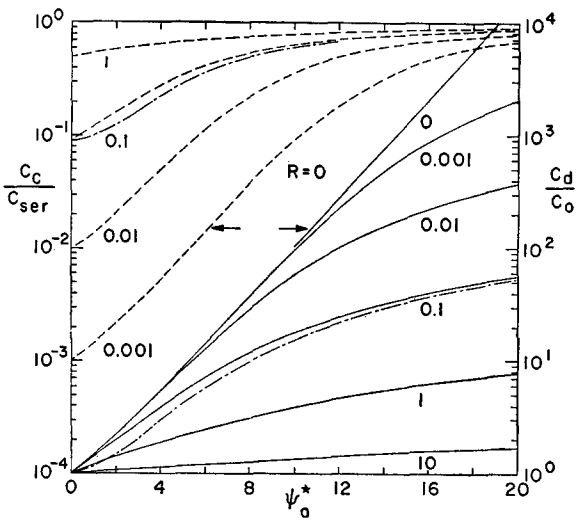

FIG. 8. Normalized space-charge differential capacitance C_d and normalized differential capacitance C_c of series combination of C_d and the capacitance C_{ser} of a charge-free region *versus* positive applied normalized potential (accumulation region formation) for various values of δ.

Figure 8 shows the dependence of C_c/C_{ser} and C_d/C_0 on total applied positive potential for $R=0$ and various δ values between 10^{-3} and 10. Although C_d/C_0 will only be directly measurable for $\delta=0$, it is presented for other δ values as well to show how the potential division of ψ^*_a into ψ^*_0 across the space-charge region and $(\psi^*_a-\psi^*_0)$ across C_{ser} retards its increase and the corresponding growth of an accumulation region. For large δ, most of the available potential appears across C_{ser} and C_d/C_0 is slow in increasing. Further, as it increases with increasing ψ^*_a, its share of ψ^*_a becomes proportionately less. The two dash-dot curves are plotted for the two-mobile case and $\delta=0.1$. They also apply to the present one-mobile case when R is large. To avoid cluttering up the graph, such curves have only been shown for $\delta=0.1$; however, the difference between the one- and two-mobile curves is still small for other δ values. It should be noted that especially when $\delta \ll 1$ the C_c/C_{ser} curves show a considerable region very little different from the C_d/C_0 curves. As ψ^*_a increases, C_c must approach C_{ser}, however, since the space-charge capacitance will eventually become so large its effect in the series combination will be negligible.

Figure 9 applies to the same situation as Fig. 8 but with ψ^*_a negative. Here $(C_c/C_{c0})^{-2}$ is plotted (solid and dash-dot lines) since this quantity may be expected to depend linearly on ψ^*_a for sufficiently negative values of ψ^*_a to produce an exhaustion region. The dashed lines in the figure are extrapolations of the final linear region. The two dash-dot curves apply to an abrupt *pn* junction.[24] For $\delta=0$, $(C_c/C_{c0})^{-2}$ becomes $(C_d/C_0)^{-2}$ which is, for such a *pn* junction, simply $[1+|\psi^*_a/\phi^*_0|]$. Here ϕ^*_0 is the normalized built-in or junction potential arising from the different doping on the two sides of the

junction. It may be obtained experimentally from the intersection of the final straight line (dashed curve) and the line $(C_c/C_{c0})^{-2}=1$. No value of ϕ^*_0 has been explicitly assumed in calculating the $(C_c/C_{c0})^{-2}$ curves for the one-mobile, blocking-electrode case, but it is evident that the theory leads to an effective value of ϕ^*_0 dependent on δ.

In calculating the *pn* junction curve for $\delta=0$, a value of ϕ^*_0 of 0.5005 has been used since this turns out to be the effective value of ϕ^*_0 for the one-mobile curve for the same δ and thus makes the final limiting portions of the curves identical. If unity is subtracted from the $(C_d/C_0)^{-2}$ expression for the *pn* junction, the result is just the dashed extrapolated straight line. For each δ value, this line has been continued down to $(C_c/C_{c0})^{-2}=0.1$ in order to show in a detailed way the deviation

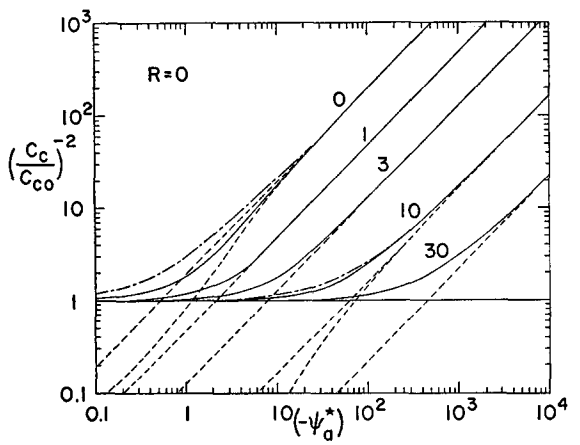

FIG. 9. Dependence of $(C_c/C_{c0})^{-2}$ on negative applied normalized potential (exhaustion region formation) for $R=0$ and various values of the capacitance ratio δ. Dash-dot lines are for abrupt *pn* junctions, solid lines for the case of charge of only one sign mobile.

between the behavior of a *pn* junction and the one-mobile solution. The dotted lines shown for $\delta=0$ and 10 are obtained by subtracting unity from the one-mobile $(C_c/C_{c0})^{-2}$ results. Since they do not approximate very closely to *pn* junction behavior in the region of the bend of the curves, the dotted and dashed lines differ from each other.

The effective value of ϕ^*_0 for the one-mobile case is 60.4 for $\delta=10$. The *pn*-junction curve for $\delta=10$ has been calculated two ways. First, it was calculated using the above value of ϕ^*_0 and taking $(C_c/C_0)^{-2}=(C_d/C_0)^{-2}$. Since $\delta=10$ here, a more pertinent method of calculating it is to use Eq. (32′) together with $\phi^*_0=0.5005$. First, C_d/C_0 is calculated, then $(C_c/C_{c0})^{-2}$. In order to carry out this procedure, C_s/C_0 for the abrupt *pn* junction is necessary. The required expression is[6]

$$C_s/C_0=2(|\phi^*_0/\psi^*_0|)^{\frac{1}{2}}[(1+|\phi^*_0/\psi^*_0|)^{\frac{1}{2}}-(|\phi^*_0/\psi^*_0|)^{\frac{1}{2}}]. \quad (28)$$

Both methods of calculating the *pn*-junction curve for $\delta=10$ gave the same results.

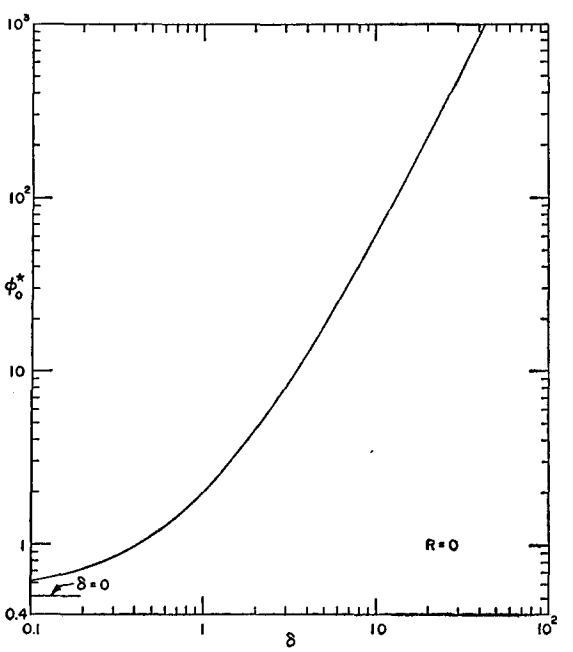

FIG. 10. Effective built-in normalized potential ϕ^*_0 arising from charge-free region as a function of δ.

Figure 10 shows how the effective ϕ^*_0 arising in the one-mobile, blocking-electrode case varies with δ. The final limiting form of the curve is $\phi^*_0=\delta^2/2$. Physically, this effective built-in potential arises in the following way. When δ is large, $C_{ser}\ll C_0$, and most of ψ^*_a appears across C_{ser} until ψ^*_a is sufficiently negative to cause C_s to decrease enough that C_s and C_{ser} are comparable in magnitude. Thereafter, as C_s decreases, a larger and larger part of ψ^*_a appears across C_s as it becomes smaller and smaller. It is thus evident that the behavior for positive and negative ψ^*_a is quite different. Comparison of theory and measurements for either polarity should allow δ, ϕ^*_0, C_0, and C_{ser} to be obtained, but greatest accuracy will be obtained when measurements with both polarities can be made and are well described by the present theory. Note that an inhomogeneous distribution of N can also change the

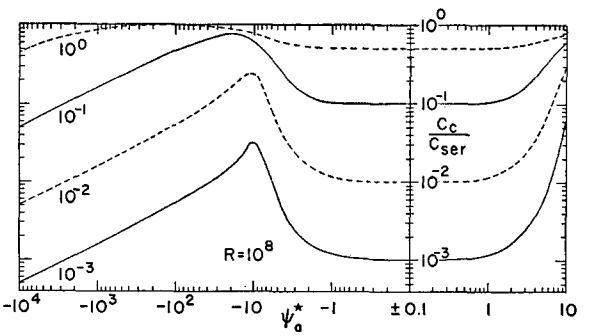

FIG. 11. (C_c/C_{ser}) *versus* positive and negative applied normalized potential for $R=10^8$ and various δ values.

shape of C_c and C_d curves, but it cannot lead to a peak in these curves as can recombination effects.

We have not yet considered in any detail curves with both δ and R greater than zero; in this case it may be difficult to sort out all the pertinent quantities accurately. In particular, it will be noted from Fig. 7 that with $\delta=0$ a value of R somewhat less than 100 could lead to an apparent ϕ^*_0 of about 3 which might be confused with the $R=0$, $\delta=1.5$ case which leads to the same ϕ^*_0 but with a somewhat different curve shape. It is probable that a number of experimental determinations of ϕ^*_0 from differential capacitance measurements might have more properly been interpreted in terms of nonzero δ or R rather than a real ϕ^*_0. Stratton[31] cites measurements of Parnell on SiC—SiC contacts where C_d or C_c remained constant up to 4 volts for either polarity. Such constancy at room temperature would require a value of an effective ϕ^*_0 of between 10^2 and 10^3. From Fig. 10, δ would therefore lie between about 13 and 40. For such a large value of δ, bias of polarity to form an accumulation layer would lead to no appreciable change in C_d/C_0, as shown by Fig. 8. Opposite bias up to about $\phi^*_0/3$ would also have little effect as one can see from Fig. 9. Of course, these results in the constant capacity region could also be explained by a Mott barrier as Stratton suggests. Such a barrier would not show a final drop off of C_c with large negative bias, however.

Finally, Fig. 11 shows the behavior of C_c/C_{ser} for $R=10^8$, various δ values, and for both positive and negative applied potential. These curves should be compared with those of Fig. 7 for $\delta=0$. For $\delta\ll1$, the shape of the present curves is very similar to that for $R=10^8$ in Fig. 7. As δ increases, the negative peak broadens, flattens, and is displaced to more negative potentials. Thus, different δ values can lead to any peak height from the maximum value obtained with $\delta=0$ to a complete washing out of a peak for δ of the order of 10 or more. The curves of Fig. 11 have been normalized with respect to C_{ser} rather than C_{c0} in order to show both the decrease in C_c as R is increased and the approach of all curves to C_{ser} as ψ^*_a increases positively. Normalization with respect to C_{c0} can be accomplished by translating all curves vertically to the same value at small ψ^*_a; the curves will then be somewhat more directly comparable with those of Fig. 7. Although the author is unaware of capacitance measurements in solids which show such strong peaks as those evident in Figs. 7 and 11, somewhat similar results have been found in electrolytes[16] and conditions suitable for their observation in solids could readily be set up, for example in insulating photoconductors, and should yield valuable information concerning recombination, the presence of charge-free layers, mobile and fixed charge concentration, etc.

[31] R. Stratton, Proc. Phys. Soc. (London) **B69**, 513 (1956).

ACKNOWLEDGMENT

The author is most grateful to J. B. Harvill for sustained aid in finding and correcting errors in the several IBM 650 computer programs required for the present work and for invaluable help in programing procedures.

GLOSSARY OF SYMBOLS

C_d	Differential space-charge capacitance per unit area.
C_s	Static space-charge capacitance per unit area.
C_0	Common value of C_d and C_s in the limit of zero potential. $C_0=\epsilon/4\pi L_e$.
C_{ser}	Constant series capacitance per unit area.
C_c	Series combination of C_{ser} and C_d.
C_{c0}	Value of C_c in the limit of zero potential.
D_n	Diffusion constant of negative charge carriers.
D_p	Diffusion constant of positive charge carriers.
e	Arithmetic value of the electronic charge.
E	Electric field strength. $E^*=E/(kT/eL_e)$.
E_0	Electric field strength at blocking electrode or at juncture of space-charge region and charge-free region.
k	Boltzmann's constant.
k_1	Dissociation constant. Probability per unit time for dissociation of neutral centers.
k_2	Recombination constant.
L_{D_1}	Debye length for mobile charges of concentration N. $L_{D_1}=[\epsilon kT/4\pi e^2N]^{\frac{1}{2}}$.
L_{D_2}	Debye length for charges of both signs mobile and concentration N. $L_{D_2}=L_{D_1}/\sqrt{2}$.
L_e	Effective value of Debye length when charges of one sign are mobile and may recombine with fixed charges of opposite sign. $L_e=\theta L_{D_1}$.
n	Concentration of negative carriers, assumed mobile. $n^*=n/N$.
n_∞	Concentration of positive and negative carriers in regions of no space charge.
n_c	Concentration of neutral centers. $n_c=N-p$.
N	Concentration of neutral centers (assumed donors) before any dissociation.
p	Concentration of positive carriers, assumed immobile. $p^*=p/N$.
q_n	Change in negative charge in the material produced by electric field.
q_p	Change in positive charge in the material produced by electric field.
q_0	Negative charge on the blocking electrode. $q_0=q_n-q_p$.
R	Dimensionless recombination ratio. $R=k_2N/k_1$.
T	Absolute temperature.
x	Distance into charge-containing material measured from blocking electrode at $x=0$. $x^*=x/L_e$.
z	Normalized distance from blocking electrode in L_{D_1} units. $z=x/L_{D_1}$.

δ Ratio of C_0 to C_{ser}.
ϵ Low-frequency limiting value of the differential dielectric constant in the absence of free charges.
θ Correction factor depending on R. $\theta=[n^*_\infty(2-n^*_\infty)]^{-\frac{1}{2}}$.
μ_n Microscopic mobility of negative charge carriers.
μ_p Microscopic mobility of positive charge carriers.
ϕ_0 Junction or built-in potential of a pn junction. $\phi^*_0=\phi/(kT/e)$.
ψ Average inner lattice potential in space-charge region. $\psi=0$ at $x=\infty$. $\psi^*=\psi/(kT/e)$.
ψ_0 Value of ψ at blocking electrode or at junction of space-charge region and charge-free region. $\psi^*_0=\psi_0/(kT/e)$.
ψ_a Sum of ψ_0 and potential drop across charge-free region when present. $\psi^*_a=\psi_a/(kT/e)$.

THE JOURNAL OF CHEMICAL PHYSICS VOLUME 29, NUMBER 6 DECEMBER, 1958

Composition of Nitrogen Oxide Equilibria

ELEONORA VAN BEEK-VISSER

Fysisk Institutt, Norges Tekniske Høgskole, Trondheim, Norway

(Received May 23, 1958)

The nitrogen oxide equilibrium is recalculated on the basis of the new spectroscopic value for the dissociation energy of nitrogen. Complete tables of the composition are given in the temperature range 2–5000°K. The maximum amount of fixed nitrogen (at 1 atmos pressure and a nitrogen oxygen ratio as in natural air) is ~5 mole percent and occurs at a temperature of ~3500°K. The influence of the N/O ratio is indicated.

INTRODUCTION

THE amount of fixed nitrogen obtainable by oxidation at high temperatures has been assessed many times both experimentally and theoretically, but the results differ rather widely. In the days of the Birkeland-Eyde process the maximum appeared to be well below 5 mole percent of fixed nitrogen, but considerably higher outputs have been reported.[1]

A preliminary calculation of A. Larsen *et al.*[2] led to a theoretical optimum near 7%, but the data were not by that time complete enough to reach a definitive conclusion. The main obstacle to an accurate determination was the well-known uncertainty in the dissociation energy of the nitrogen molecule. Since the latter problem now is resolved, a complete thermodynamical calculation on the basis of spectroscopical data is possible, the result of which is here presented.

1. SELECTION OF THE SPECTROSCOPIC DATA

1.1 O_2

The ground state of O_2 is $^3\Sigma$ and there are no other low lying electronic terms. Therefore the statistical weight is 3. The symmetry number is evidently 2. The vibration energy is given in the form,[3]

$$E_{vibr}=hc\{\omega_e(n+\tfrac{1}{2})+x_e(n+\tfrac{1}{2})^2+\cdots\} \quad (n=0,1\cdots),$$
$$=\text{const}+n\cdot hc\omega+n^2\cdots \quad (1)$$

with

$$\omega=\omega_e-x_e\omega_e. \quad (2)$$

In the sum over states we take only into account the terms linear in ω, and have therefore to choose $\nu=\omega_e(1-x_e)/c$. For O_2 also the moment of inertia and the dissociation energy $D=2\epsilon^0_{atom}-\epsilon^0_{molecule}$ are known with great accuracy.

In all we have from Herzberg's tables:

$$g_{O_2}=3 \qquad \sigma_{O_2}=2 \qquad \omega_{O_2}=1568.29\ \text{cm}^{-1}$$
$$I_{O_2}=19.13\cdot10^{-40}\ \text{g cm}^2 \qquad D_{O_2}=5.115\ \text{ev}.$$

1.2 N_2

The ground state of the N_2 molecules is $^1\Sigma$, hence $g=1$. Likewise the band constants ω_e, x_e, and the moment of inertia have been accurately known for a long time. But as mentioned before, the dissociation energy has been the subject of much debate. Still in 1951 Douglas and Herzberg[4] could not make a choice between the values 9.756 and 7.373 ev, and distinguished spectroscopists[5] were even advocating the low value 5.0 ev. From measurements of the temperature of the cyanogen oxygen flame Thomas, Gaydon, and Brewer[6] concluded that the highest value 9.76 ev was the correct one, and this is also in agreement with experiments done in 1957 by Brook and Kaplan[7] and by Hendrie[8] as well as

[1] W. J. Cotton, J. Electrochem. Soc. **34a**, 489 (1947).
[2] Larsen, Torgersen, Wang, and Wergeland, Kgl. Norske Videnskab. Selskabs Forh. **27**, 156 (1954).
[3] G. Herzberg, *Spectra of Diatomic Molecules* (D. Van Nostrand Company Inc., Princeton, New Jersey, 1951), second edition, p. 92.
[4] A. E. Douglas and G. Herzberg, Can. J. Phys. **29**, 294 (1951).
[5] R. F. Schmidt and L. Gerö, Proc. Phys. Soc. (London) **60**, 533 (1948).
[6] Thomas, Gaydon, and Brewer, J. Chem. Phys. **20**, 369 (1952).
[7] M. Brook and J. Kaplan, Phys. Rev. **96**, 1540 (1954).
[8] J. M. Hendrie, J. Chem. Phys. **22**, 1503 (1954).